Supplementary Information

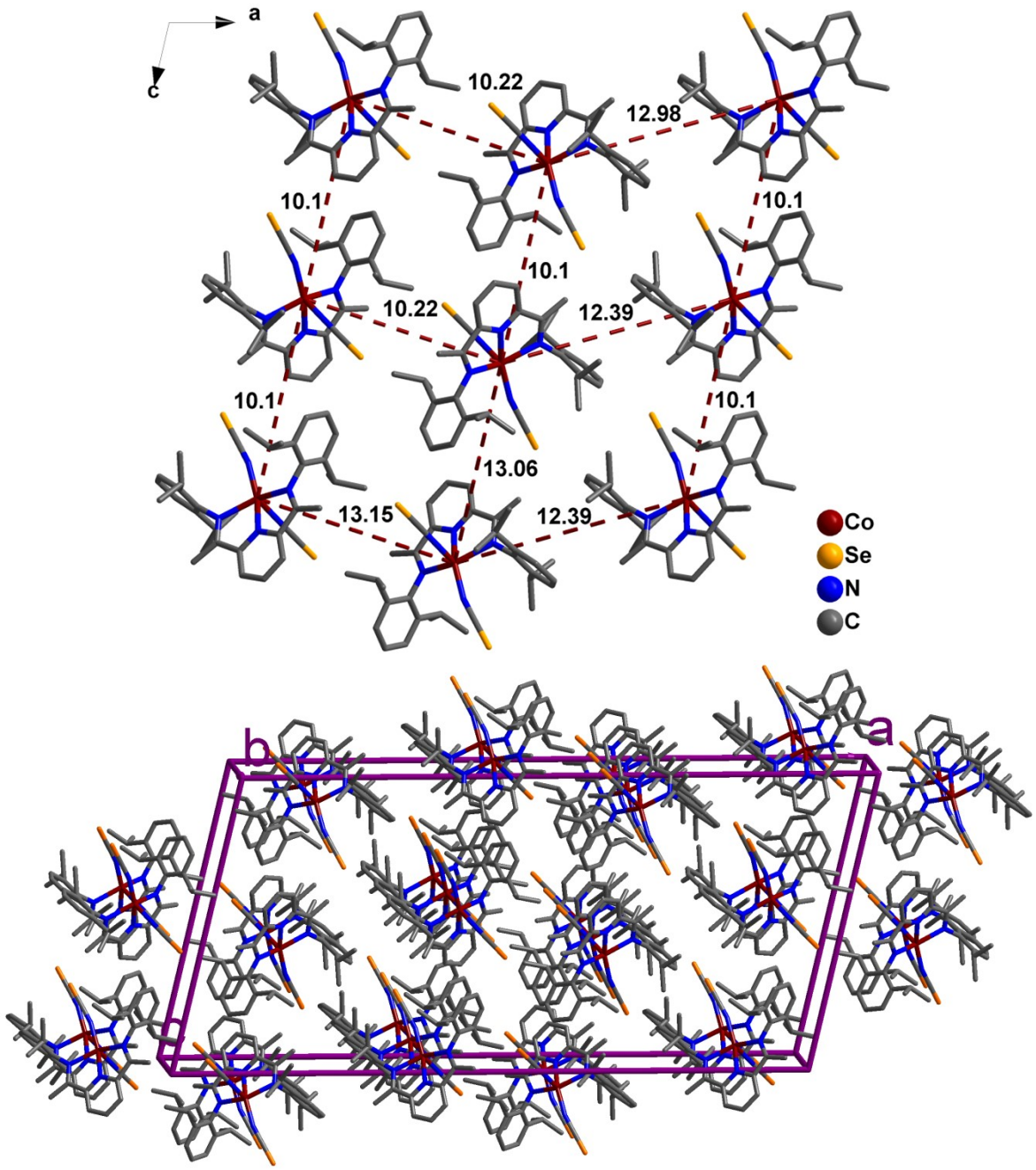

Figure S1(A). Simplified packing diagrams for complex **1** showing the shortest intermolecular $Co^{II}\cdots Co^{II}$ distances (in Å) (top) and packing diagram (bottom).

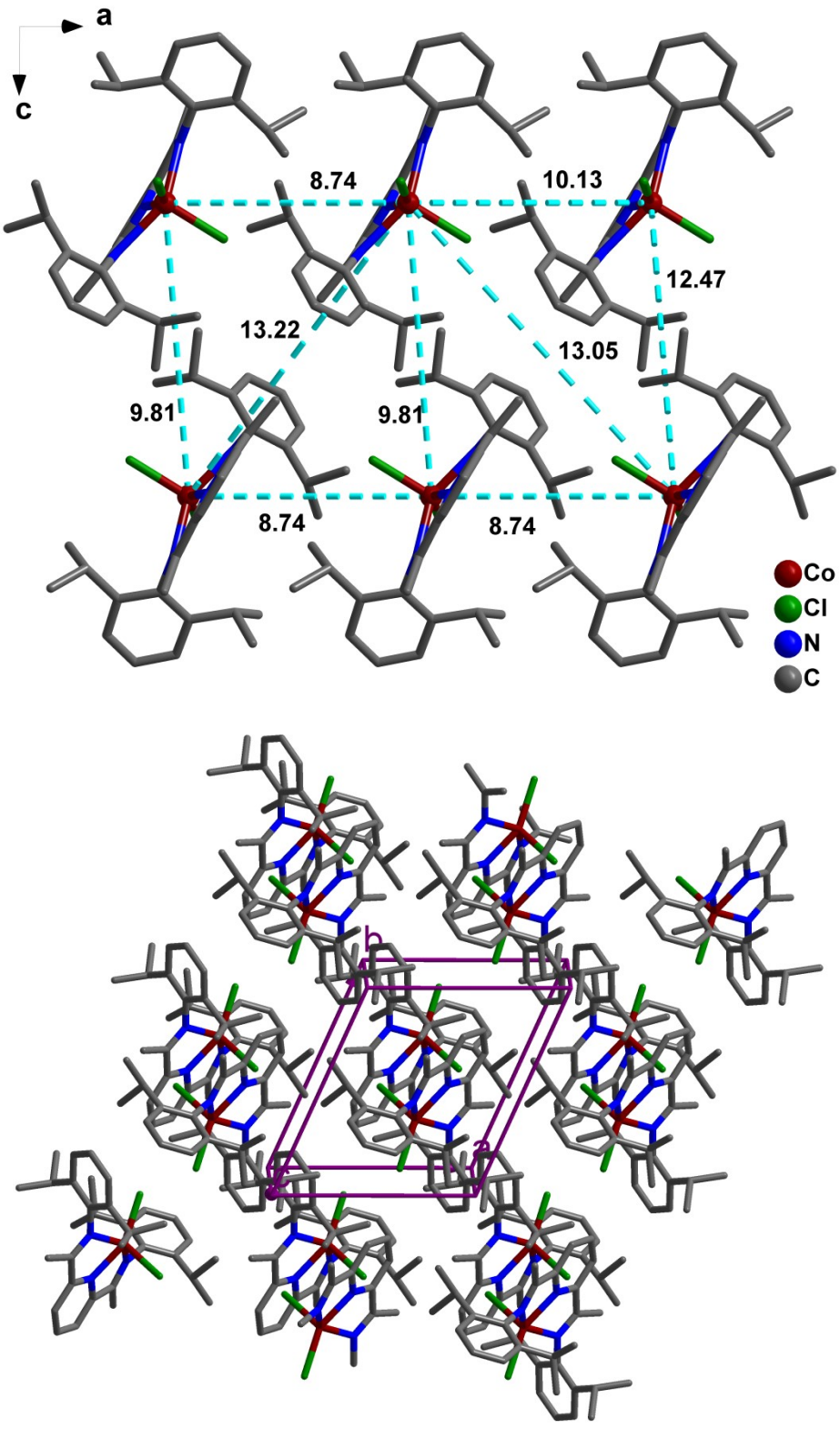

Figure S1(B). Simplified packing diagrams for complex **2** showing the shortest intermolecular $Co^{II}\cdots Co^{II}$ distances (in Å) (top) and packing diagram (bottom).

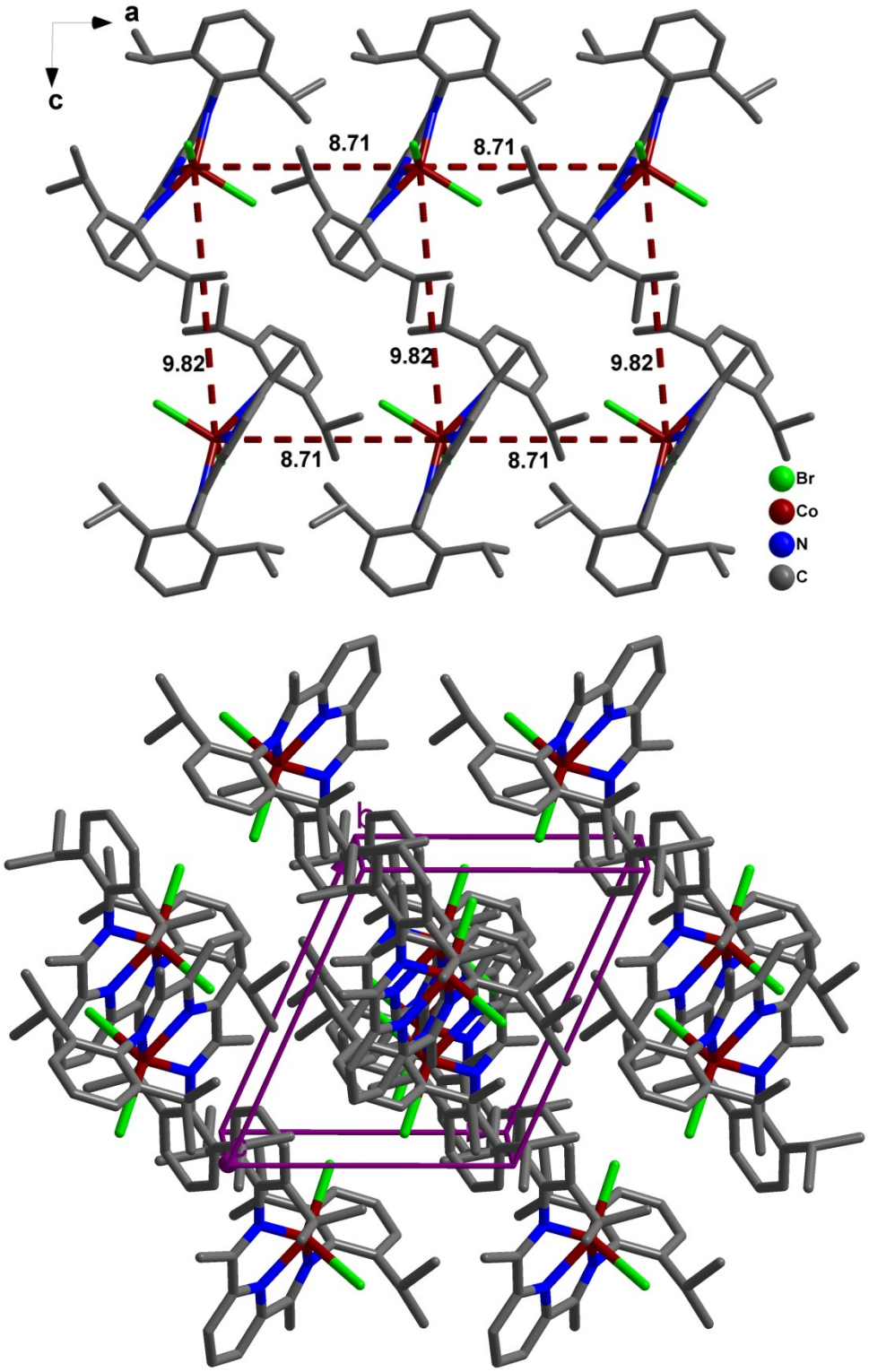
a
c
8.71
8.71
9.82
9.82
9.82
8.71
8.71
Br
Co
N
C
b

Figure S1(C). Simplified packing diagrams for complex **3** showing the shortest intermolecular $Co^{II}\cdots Co^{II}$ distances (in Å) (top) and packing diagram (bottom).

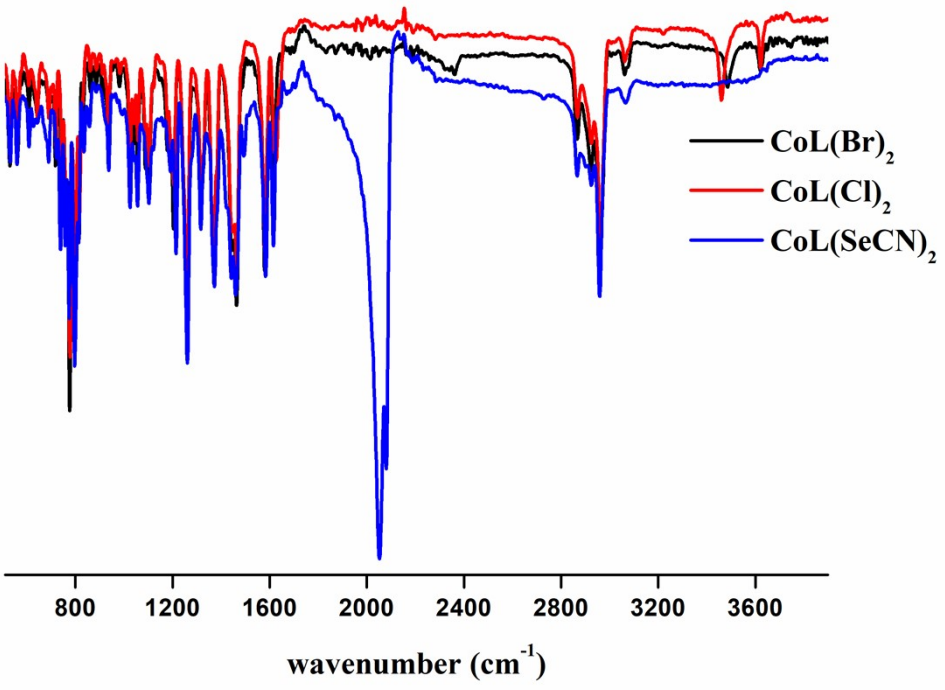

Figure S2. FTIR spectra for complexes **1**−**3**.

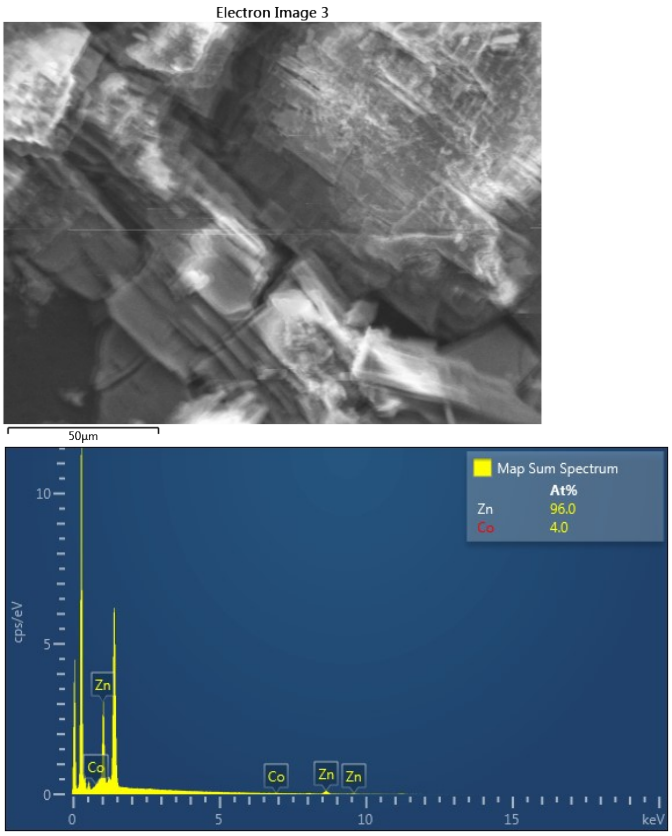

Figure S3. SEM-EDX analysis for diamgentically diluted **$[Zn^{II}_{0.96}Co^{II}_{0.04}(L)(NCSe)_2]$**.

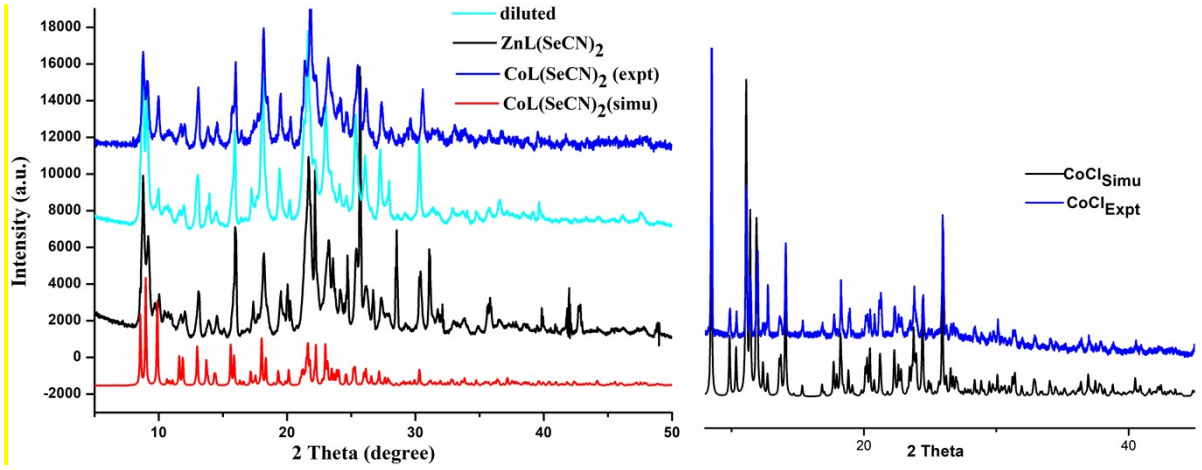

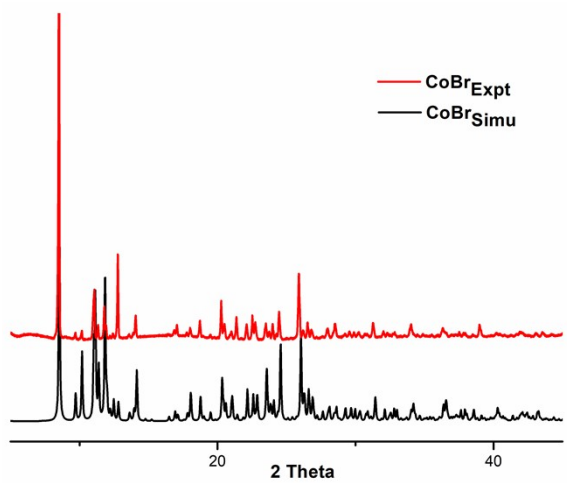

Figure S4. PXRD analysis for the diamgetically diluted [$Zn^{II}_{0.96}Co^{II}_{0.04}(L)(NCSe)_2$] (top left), complex **2** (top right) and complex **3** (bottom).

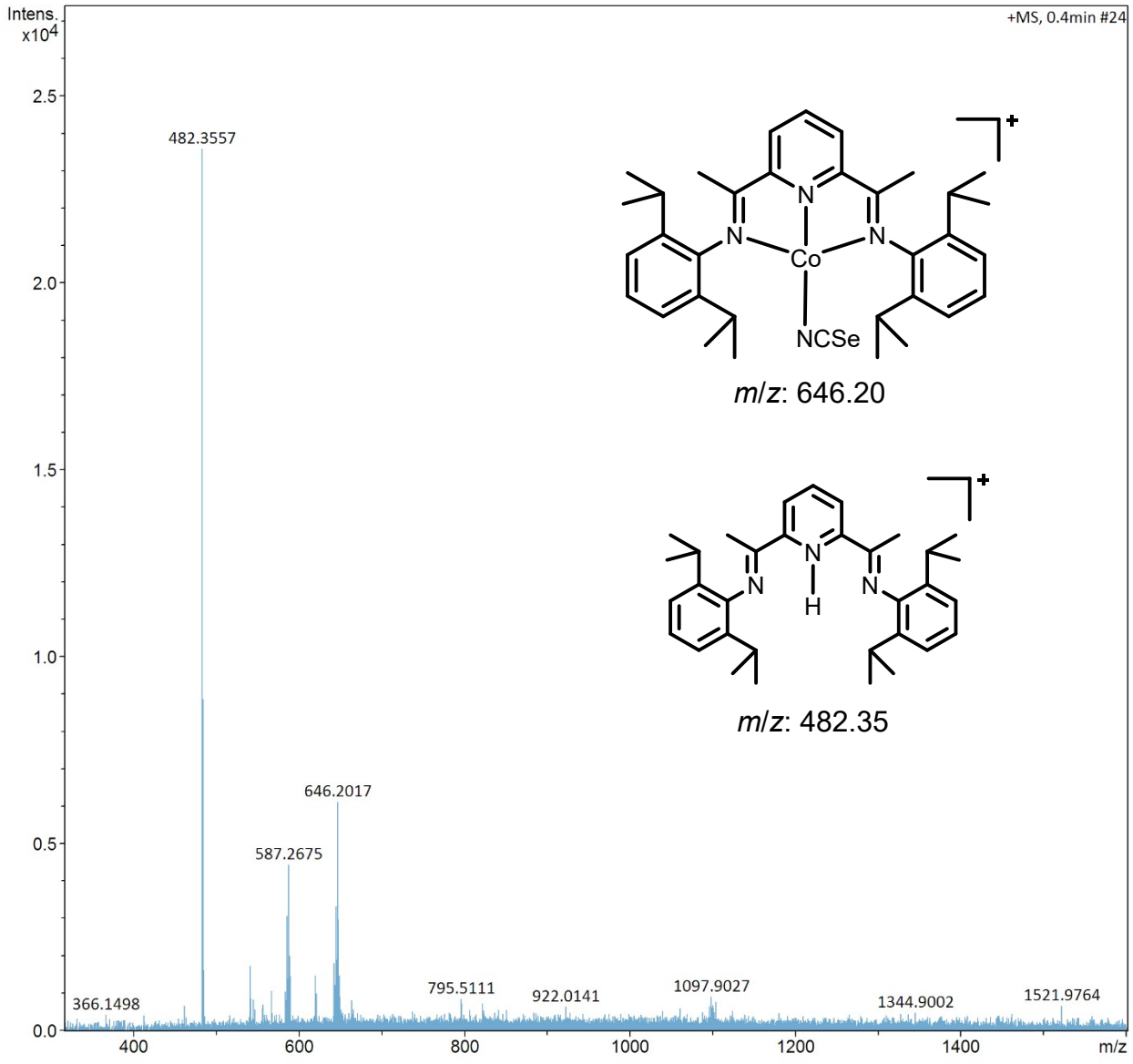

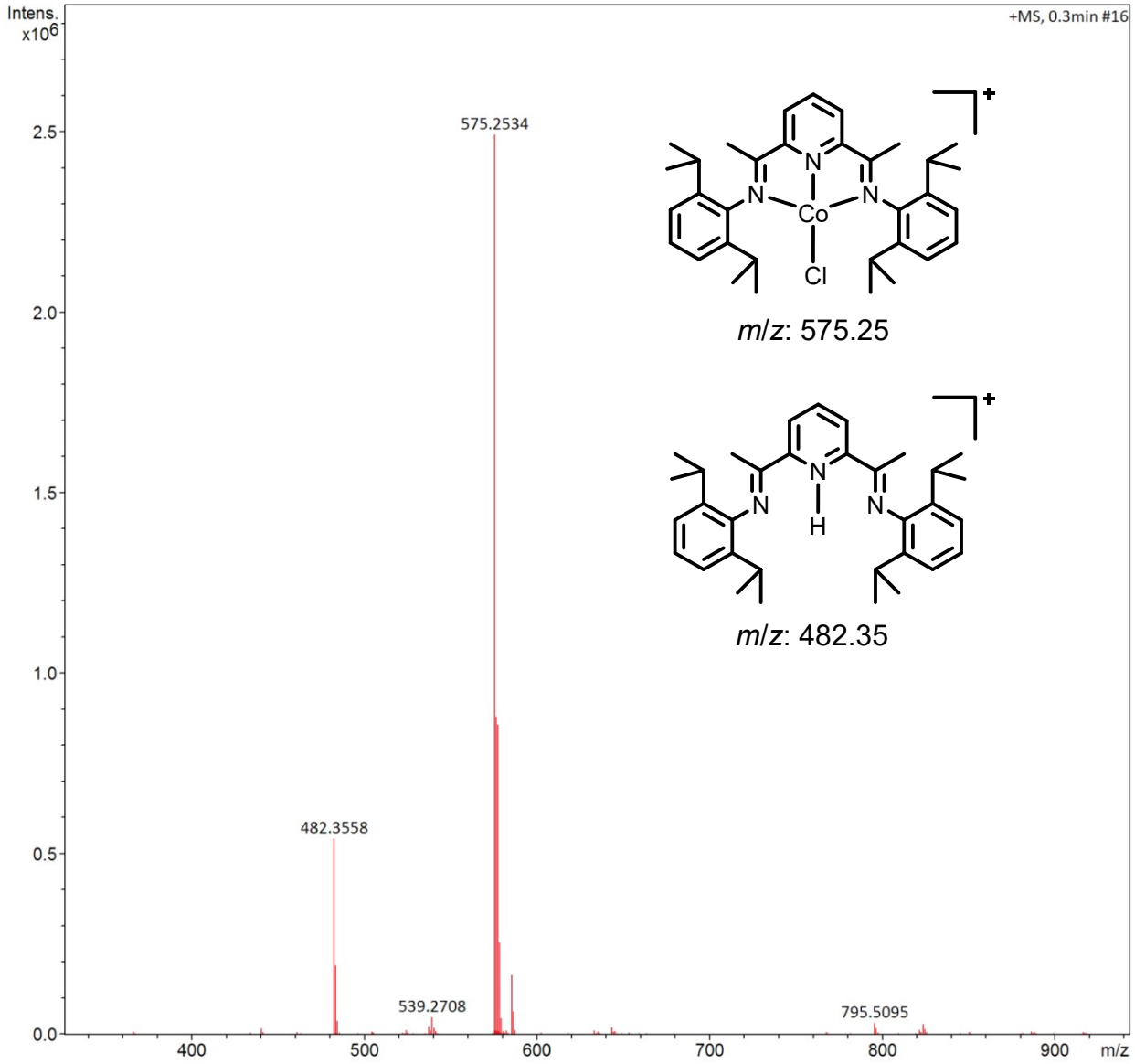
Intens.
x10^6
+MS, 0.3min #16
2.5
2.0
1.5
1.0
0.5
0.0
575.2534
482.3558
539.2708
795.5095
400
500
600
700
800
900
m/z
N
N
Co
N
Cl
+
m/z: 575.25
N
N
H
N
+
m/z: 482.35

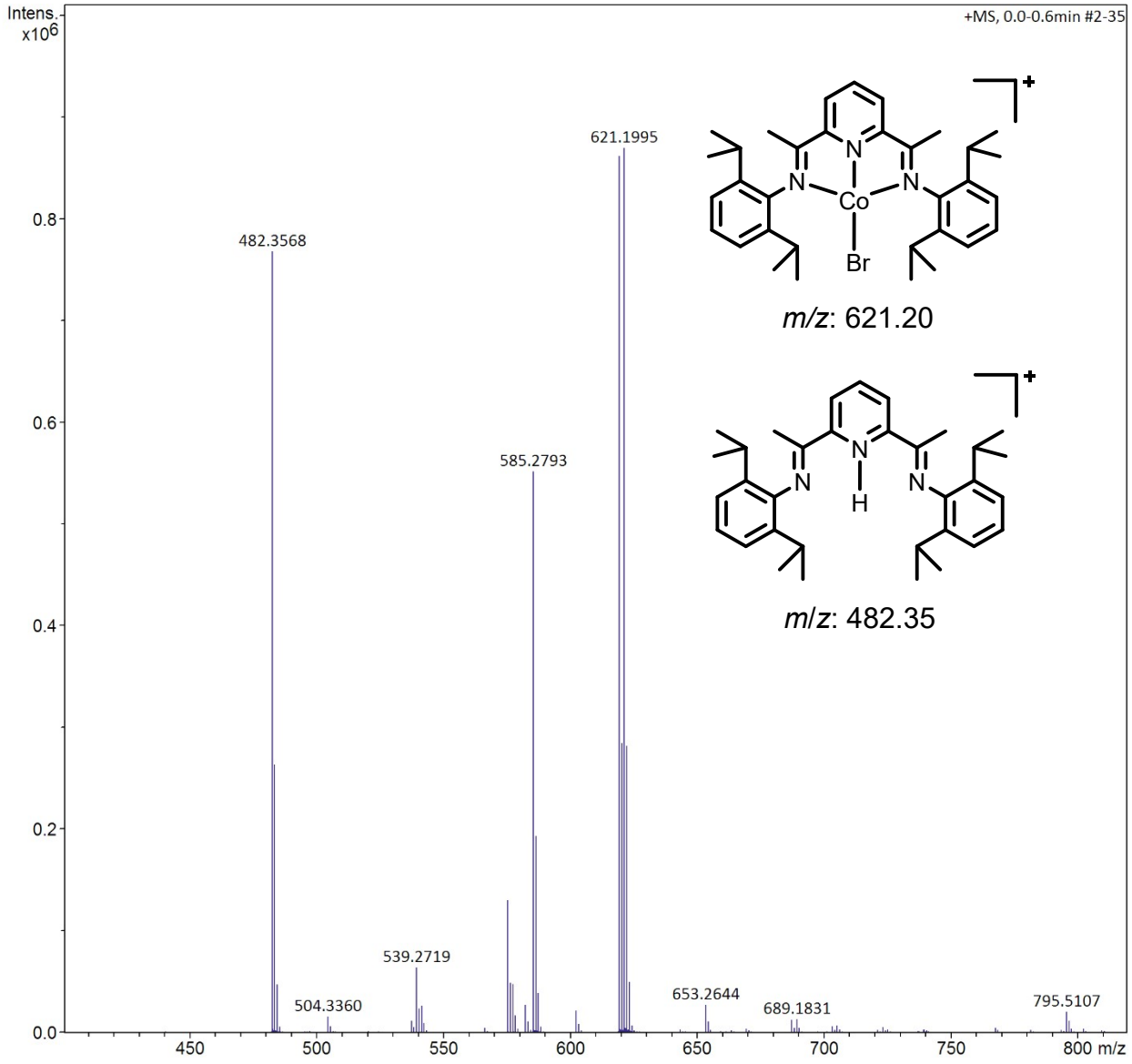

Figure S5. Mass spectra analysis data for complexes **1**−**3**.

Table S1. CShM valuesfor**1**–**3**and reported $\mathbf{4_{Me}}$ and $\mathbf{5_{Ph}}$.

PP-5 1 D5h Pentagon

vOC-5 2 C4v Vacant octahedron

TBPY-5 3 D3h Trigonalbipyramid

SPY-5 4 C4v Spherical square pyramid

JTBPY-5 5 D3h Johnson trigonalbipyramid J12

Complexes	PP-5 D5h	vOC-5 C4v	TBPY-5 D3h	SPY-5 C4v	JTBPY-5 D3h
SeCN	32.792	2.21	6.463	1.592	9.028
Cl	34.157	3.821	6.847	1.811	9.973
Br	34.446	4.414	7.188	2.219	10.115
$\mathbf{4}_{\mathbf{Me}}$	32.362	2.256	6.402	1.625	9.154
$\mathbf{5}_{\mathbf{Ph}}$	33.691	2.926	4.656	1.675	6.012

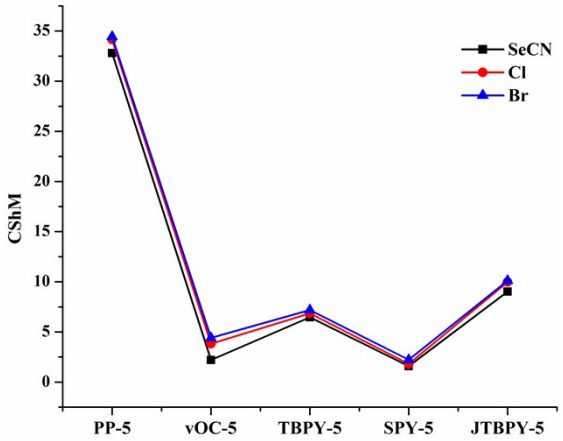

Figure S6. Plot of all the possible geometries for five coordination against the corresponding *CShM* values obtained from the SHAPE measurement for complexes **1**–**3.**

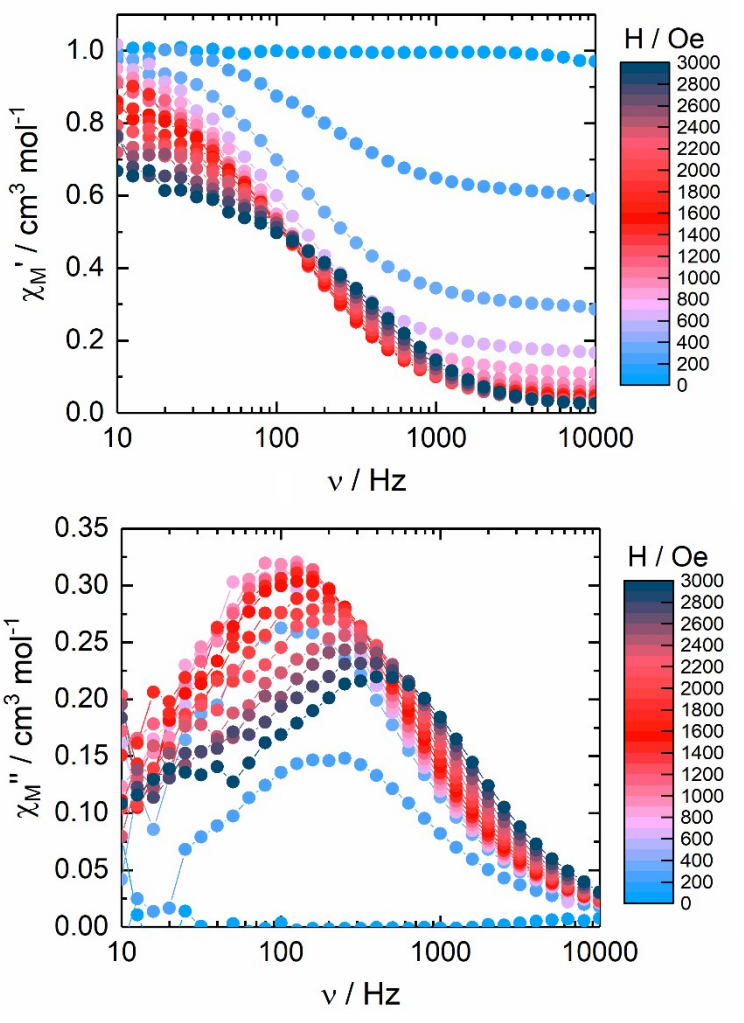

Figure S7. In-phase (top) and out-of-phase (bottom) components of the ac magnetic susceptibility for **1** at 2 K under a DC magnetic field from 0 to 3000 Oe.

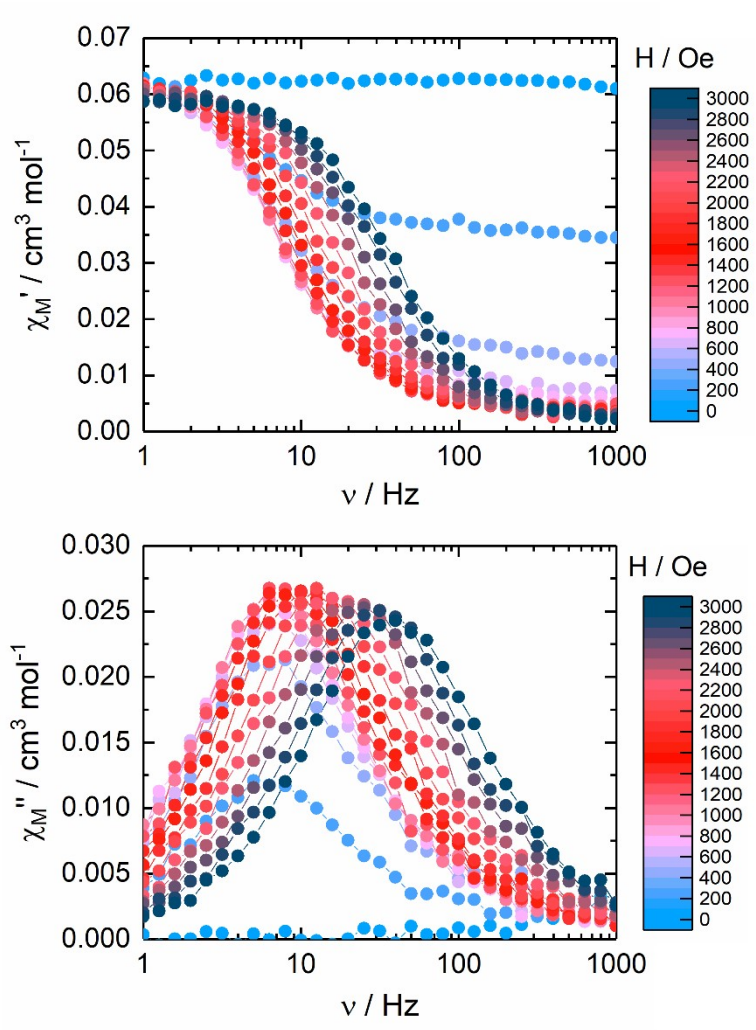

Figure S8. In-phase (top) and out-of-phase (bottom) components of the ac magnetic susceptibility for **1@Zn** at 2 K under a DC magnetic field from 0 to 3000 Oe.

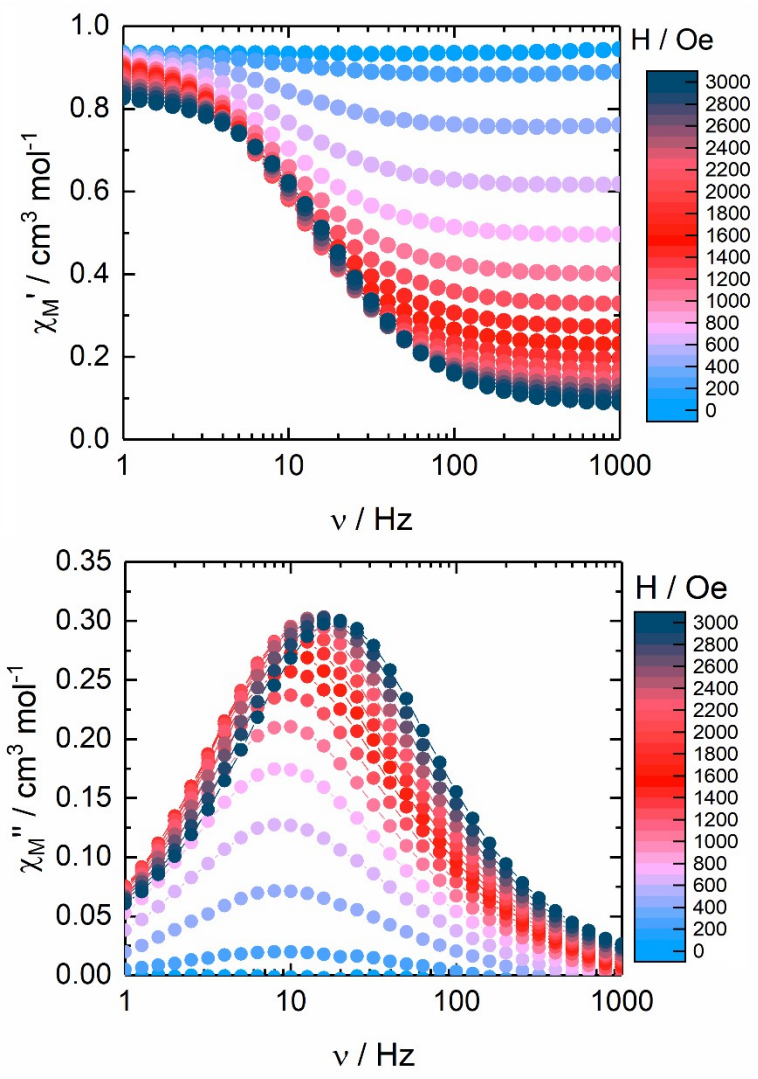

Figure S9. In-phase (top) and out-of-phase (bottom) components of the ac magnetic susceptibility for **2** at 2 K under a DC magnetic field from 0 to 3000 Oe.

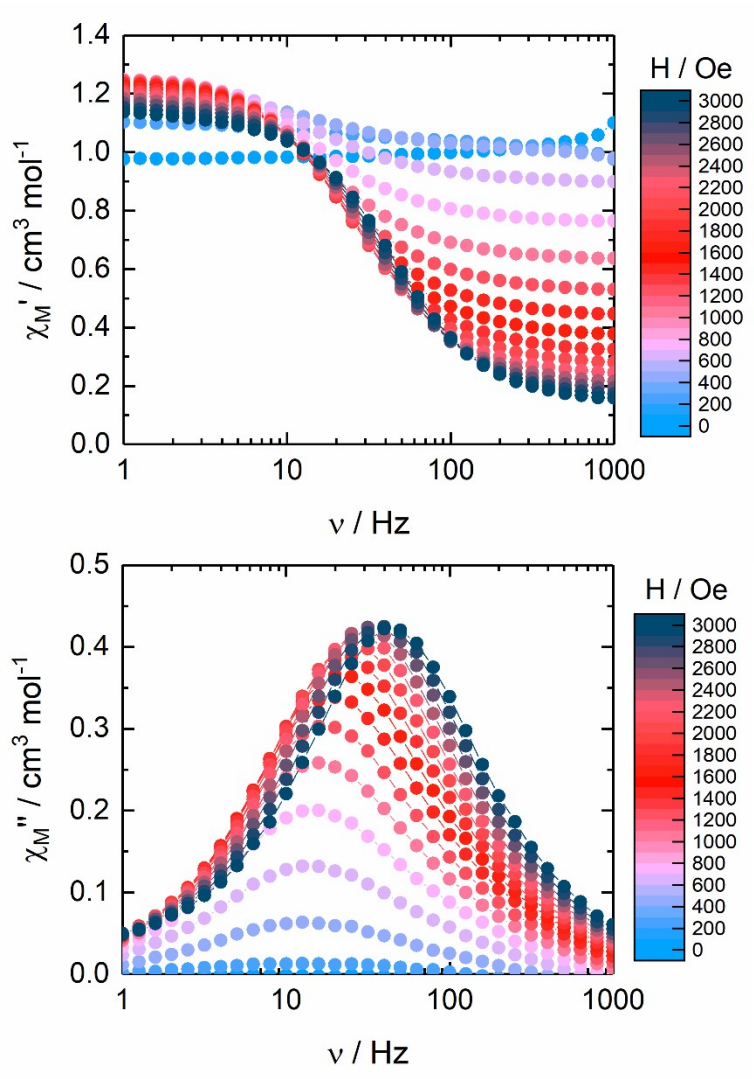

Figure S10. In-phase (top) and out-of-phase (bottom) components of the ac magnetic susceptibility for **3** at 2 K under a DC magnetic field from 0 to 3000 Oe.

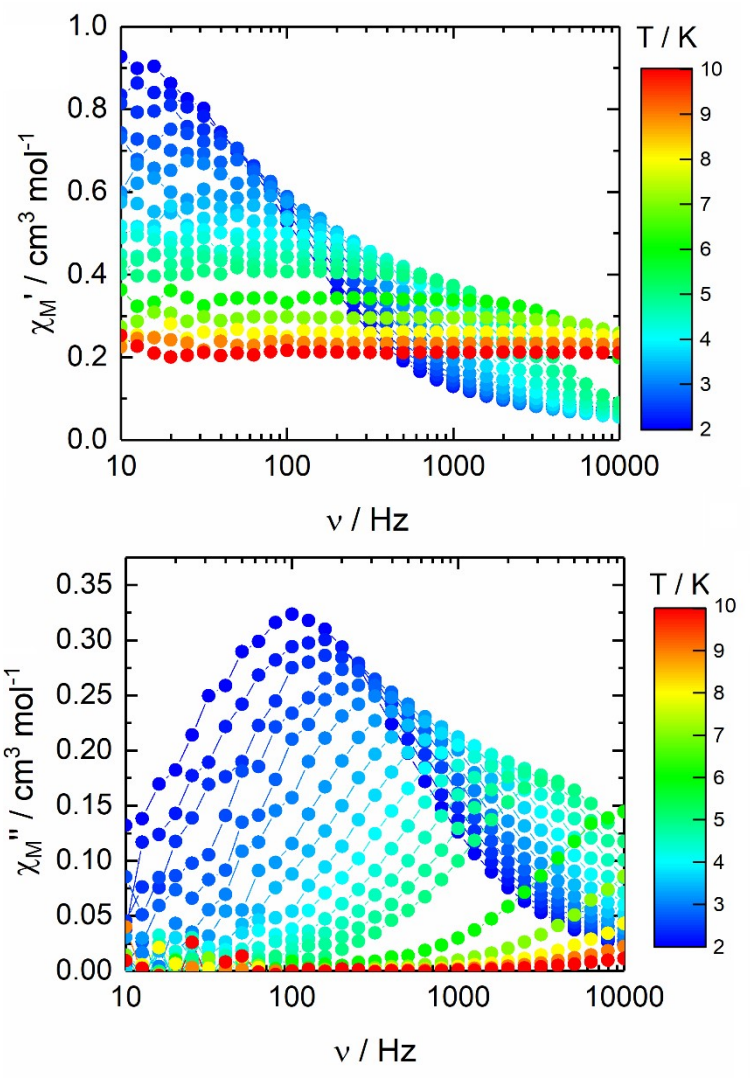

Figure S11. Frequency dependence of the in-phase (top) and out-of-phase (bottom) component of the magnetic susceptibility under an applied magnetic field of 1000 Oe between 2 and 10 K for **1**.

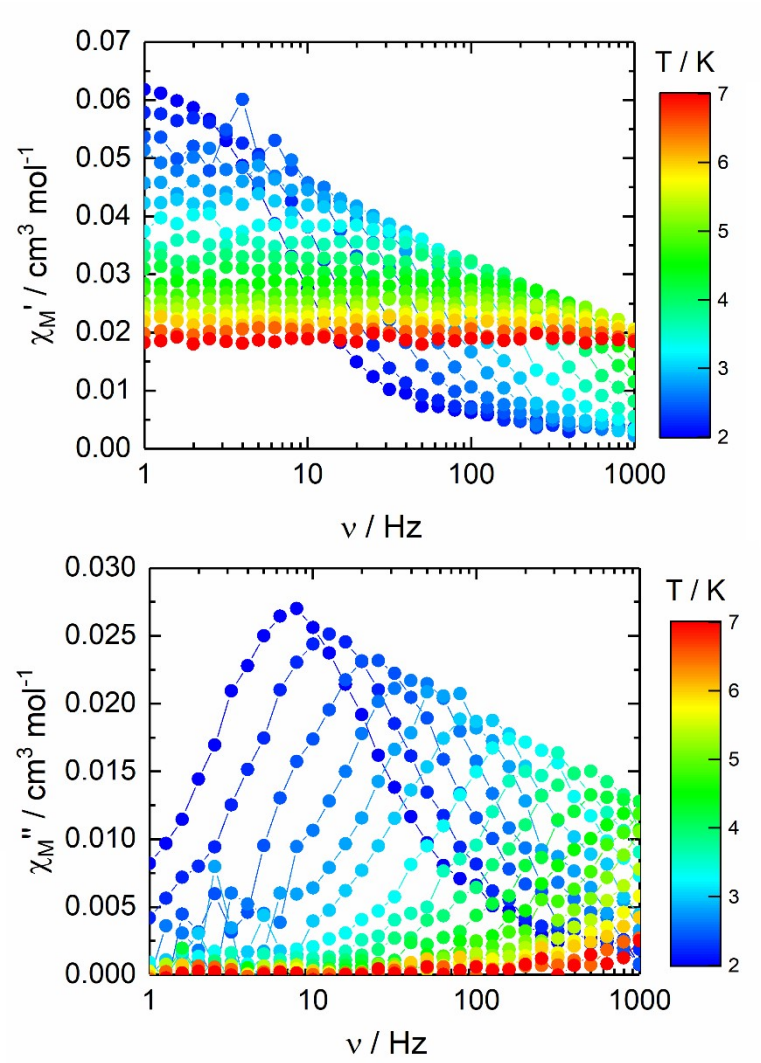

Figure S12. Frequency dependence of the in-phase (top) and out-of-phase (bottom) component of the magnetic susceptibility under an applied magnetic field of 1200 Oe between 2 and 7 K for **1@Zn**.

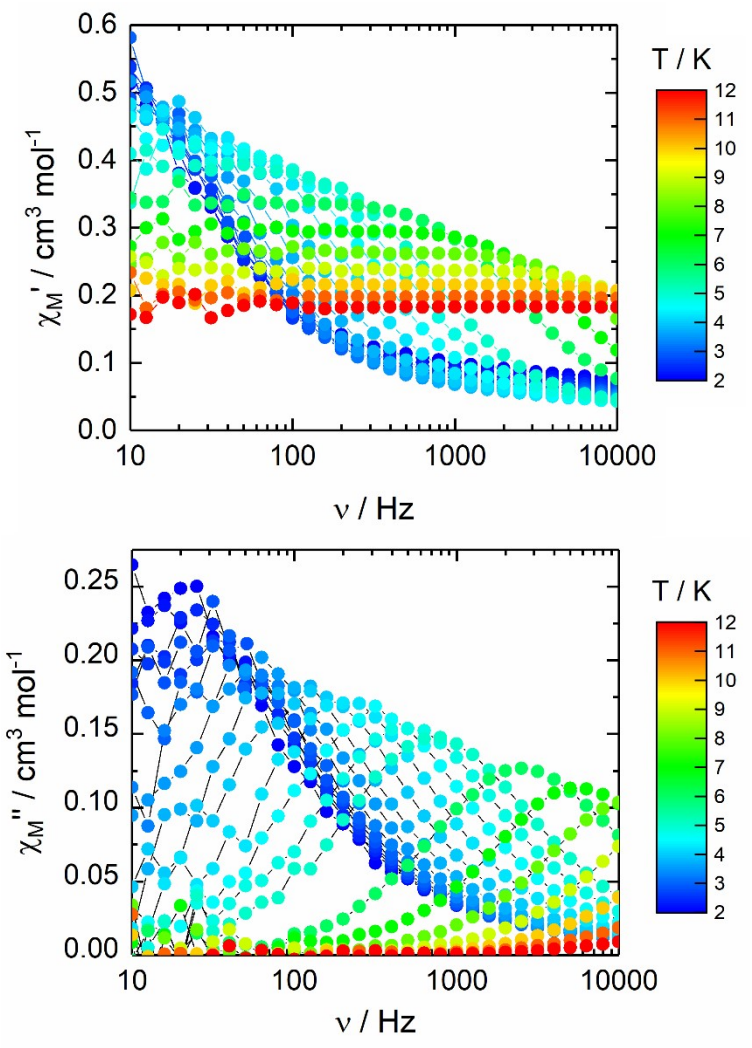

Figure S13. Frequency dependence of the in-phase (top) and out-of-phase (bottom) component of the magnetic susceptibility under an applied magnetic field of 3000 Oe between 2 and 12 K for **2**.

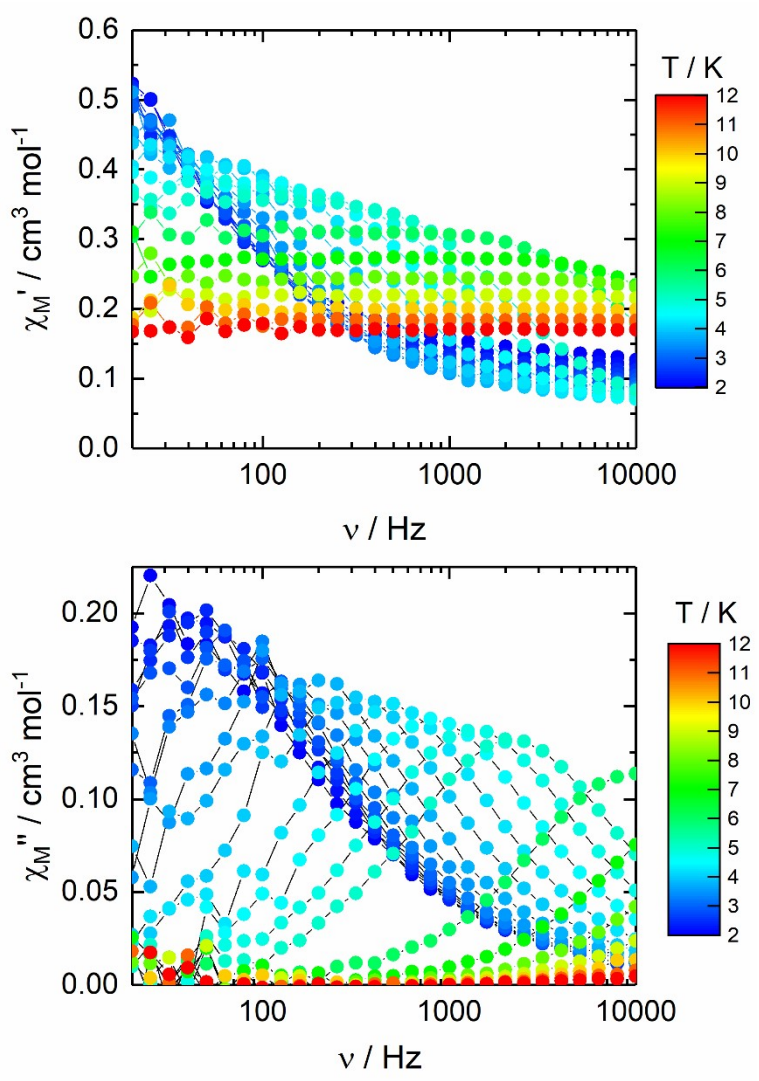

Figure S14. Frequency dependence of the in-phase (top) and out-of-phase (bottom) component of the magnetic susceptibility under an applied magnetic field of 3000 Oe between 2 and 12 K for **3**.

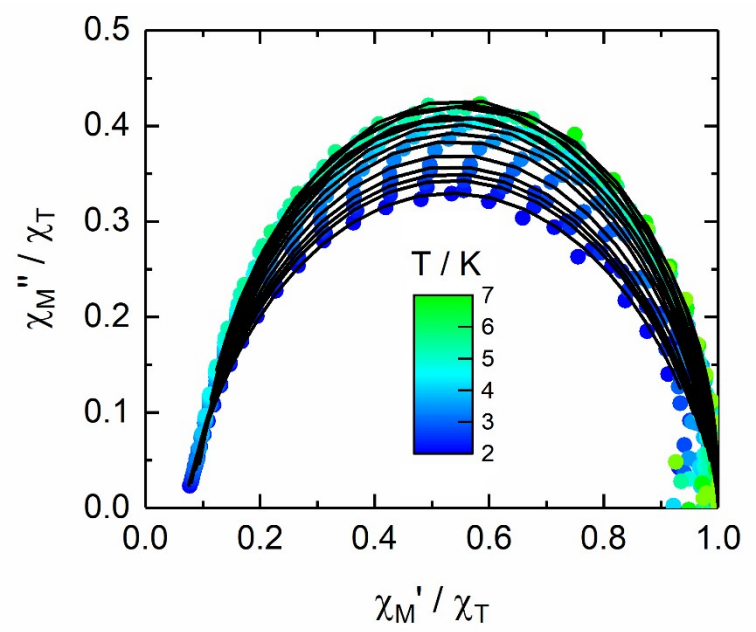

Figure S15. Normalized Cole-Cole plot for **1** at several temperatures between 2 and 7 K under an applied magnetic field of 1000 Oe. Black lines are the best fitted curves.

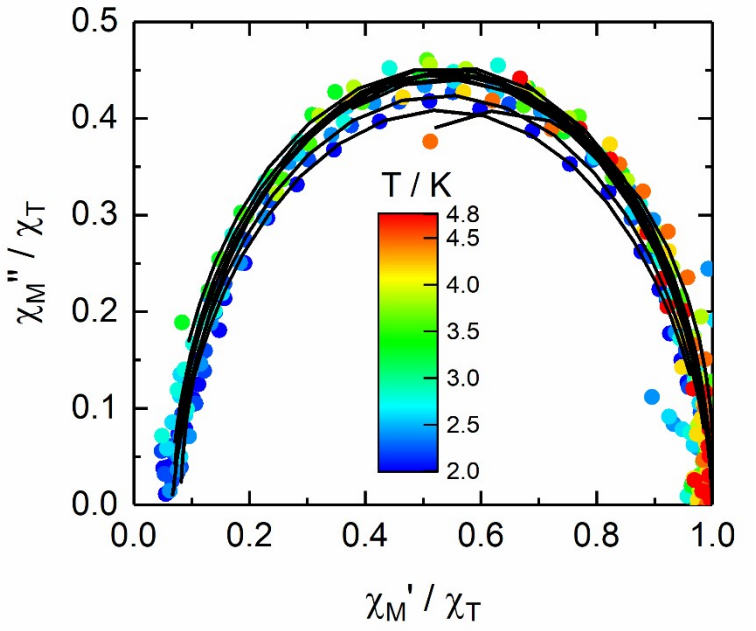

Figure S16. Normalized Cole-Cole plot for **1@Zn** at several temperatures between 2 and 4.8 K under an applied magnetic field of 1200 Oe. Black lines are the best fitted curves.

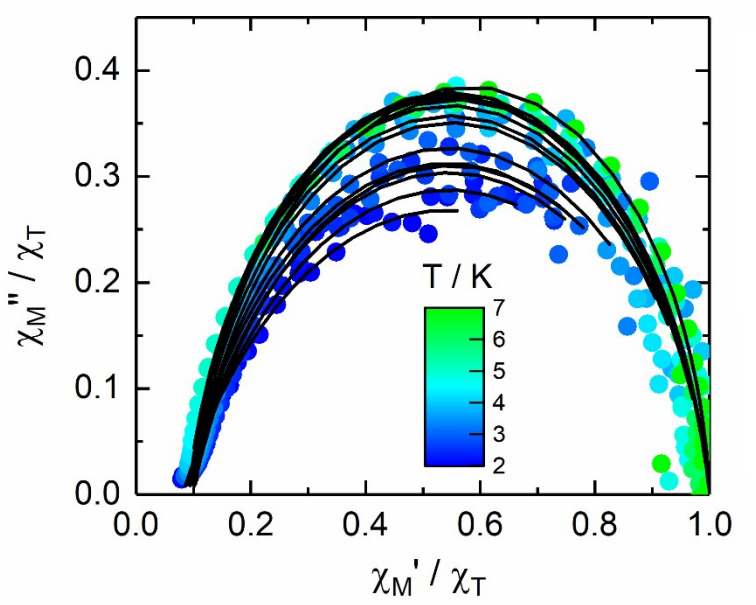

Figure S17. Normalized Cole-Cole plot for **2** at several temperatures between 2 and 7 K under an applied magnetic field of 3000 Oe. Black lines are the best fitted curves.

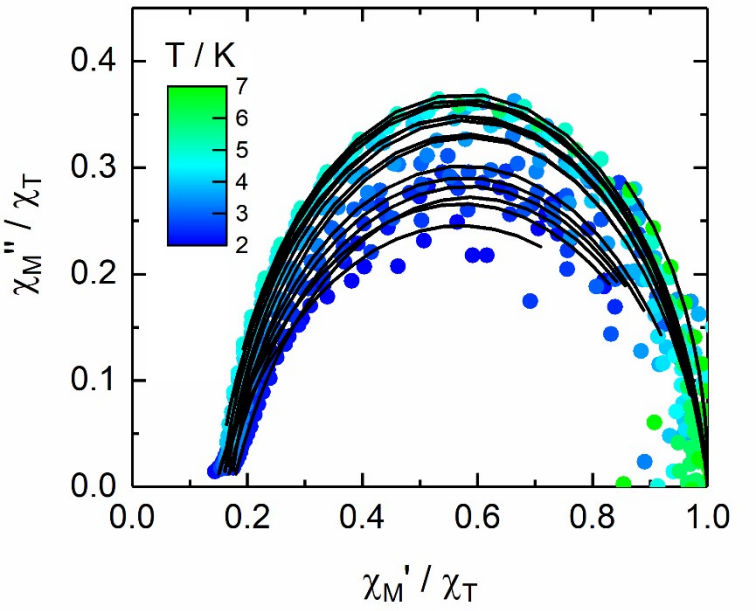

Figure S18. Normalized Cole-Cole plot for **3** at several temperatures between 2 and 7 K under an applied magnetic field of 3000 Oe. Black lines are the best fitted curves.

Extended Debye model.

$$\chi_M' = \chi_S + (\chi_T - \chi_S)\frac{1+(\omega\tau)^{1-\alpha}\sin\left(\alpha\frac{\pi}{2}\right)}{1+2(\omega\tau)^{1-\alpha}\sin\left(\alpha\frac{\pi}{2}\right)+(\omega\tau)^{2-2\alpha}}$$

$$\chi_M'' = (\chi_T - \chi_S)\frac{(\omega\tau)^{1-\alpha}\cos\left(\alpha\frac{\pi}{2}\right)}{1+2(\omega\tau)^{1-\alpha}\sin\left(\alpha\frac{\pi}{2}\right)+(\omega\tau)^{2-2\alpha}}$$

With χ_T the isothermal susceptibility, χ_S the adiabatic susceptibility, τ the relaxation time and α an empiric parameter which describe the distribution of the relaxation time. For SMM with only one relaxing object α is close to zero. The extended Debye model was applied to fit simultaneously the experimental variations of χ_M' and χ_M'' with the frequency ν of the oscillating field ($\omega = 2\pi\nu$). Typically, only the temperatures for which a maximum on the χ'' *vs. f* curves, have been considered. The best fitted parameters τ, α, χ_T, χ_S are listed in Tables S2-S9 with the coefficient of determination R^2.

Table S2. Best fitted parameters (χ_T, χ_S, τ and α) with the extended Debye model for compound **1** at 2 K in the magnetic field range 200-3000 Oe.

H / Oe	χ_S / cm^3 mol^{-1}	χ_T / cm^3 mol^{-1}	τ / s	α	R^2
200	0.60315	0.99838	7.80302E-4	0.15072	0.99907
400	0.2859	1.01403	0.00125	0.19661	0.99905
600	0.15679	1.03737	0.00157	0.22194	0.99807
800	0.09934	1.00342	0.00159	0.21113	0.9996
1000	0.06716	0.96896	0.00151	0.20807	0.99938
1200	0.04112	0.98223	0.00155	0.24148	0.99873
1400	0.02599	0.97138	0.0015	0.2541	0.99774
1600	0.02411	0.90127	0.00125	0.22082	0.99903
1800	0.0119	0.89282	0.0012	0.25136	0.99843
2000	0.00707	0.84059	0.00104	0.24699	0.99772
2200	0.01548	0.75152	7.79338E-4	0.18626	0.99923
2400	0.01218	0.70418	6.60142E-4	0.18504	0.99905
2600	0.01071	0.66938	5.66104E-4	0.17972	0.99895
2800	0.00708	0.64024	4.93266E-4	0.18787	0.99831
3000	0.00524	0.60518	4.17821E-4	0.18824	0.99813

Table S3. Best fitted parameters (χ_T, χ_S, τ and α) with the extended Debye model for compound **1@Zn** at 2 K in the magnetic field range 200-3000 Oe.

H / Oe	χ_S / cm^3 mol^{-1}	χ_T / cm^3 mol^{-1}	τ / s	α	R^2

200	0.03537	0.06382	0.02219	0.12579	0.99896
400	0.01375	0.06542	0.02269	0.14729	0.99612
600	0.00805	0.0646	0.02309	0.10615	0.99781
800	0.00628	0.06426	0.02309	0.08848	0.99876
1000	0.00509	0.06423	0.02198	0.08253	0.99866
1200	0.00451	0.06395	0.02065	0.07768	0.99842
1400	0.00402	0.06346	0.01822	0.06951	0.99876
1600	0.00356	0.06297	0.01583	0.06999	0.99888
1800	0.00358	0.06256	0.01366	0.06426	0.99897
2000	0.00321	0.06222	0.01143	0.07047	0.99931
2200	0.00299	0.06167	0.00939	0.07433	0.99905
2400	0.00283	0.06095	0.00758	0.07319	0.99936
2600	0.00257	0.06061	0.00622	0.08008	0.99933
2800	0.00231	0.06	0.00498	0.09464	0.99926
3000	0.00199	0.05936	0.0041	0.098	0.99948

Table S4. Best fitted parameters (χ_T, χ_S, τ and α) with the extended Debye model for compound **2** at 2 K in the magnetic field range 200-3000 Oe.

H / Oe	χ_S / cm^3 mol^{-1}	χ_T / cm^3 mol^{-1}	τ / s	α	R^2
200	0.88567	0.93101	0.01713	0.00944	0.99982
400	0.75752	0.93318	0.01685	0.10686	0.99983
600	0.61577	0.93612	0.01723	0.13133	0.99985
800	0.49467	0.93768	0.01714	0.14208	0.99987
1000	0.39976	0.93676	0.01658	0.14705	0.99987
1200	0.3268	0.93453	0.01582	0.15104	0.99985
1400	0.27094	0.93066	0.01527	0.15287	0.99985
1600	0.22758	0.92486	0.01476	0.15211	0.99984
1800	0.19347	0.91725	0.01406	0.14916	0.99985
2000	0.1666	0.90804	0.01319	0.14558	0.99987
2200	0.14421	0.8968	0.01219	0.14255	0.9999
2400	0.12596	0.88511	0.01118	0.14094	0.99993
2600	0.10971	0.87282	0.01017	0.14251	0.99997
2800	0.09565	0.86053	0.00924	0.14601	0.99998
3000	0.08159	0.84734	0.00836	0.15193	0.99999

Table S5. Best fitted parameters (χ_T, χ_S, τ and α) with the extended Debye model for compound **3** at 2 K in the magnetic field range 400-3000 Oe.

H / Oe	χ_S / cm^3 mol^{-1}	χ_T / cm^3 mol^{-1}	τ / s	α	R^2
400	1.03987	1.18929	0.01132	0.05768	0.99996
600	0.91156	1.24629	0.01058	0.12522	0.99995
800	0.76875	1.26113	0.00998	0.12079	0.99988

1000	0.63991	1.26361	0.00928	0.11551	0.99987
1200	0.53366	1.25988	0.00846	0.1109	0.99985
1400	0.44858	1.25356	0.0077	0.10873	0.99983
1600	0.38028	1.24416	0.00706	0.1047	0.99983
1800	0.32494	1.23309	0.00652	0.10112	0.99986
2000	0.28026	1.22045	0.00598	0.09789	0.99989
2200	0.24262	1.20661	0.00546	0.09677	0.99993
2400	0.21201	1.19058	0.00494	0.09703	0.99992
2600	0.18517	1.17365	0.00446	0.09912	0.99992
2800	0.16292	1.15588	0.00402	0.10261	0.99991
3000	0.1428	1.13774	0.00362	0.10785	0.99985

Table S6. Best fitted parameters (χ_T, χ_S, τ and α) with the extended Debye model for compound **1** at 1000Oe in the temperature range 2-7 K.

T / K	χ_S / cm^3 mol^{-1}	χ_T / cm^3 mol^{-1}	α	τ / s	R^2
2	0.06531	0.98463	0.21693	0.00156	0.99964
2.2	0.06333	0.89508	0.19011	0.00117	0.99874
2.4	0.05952	0.83391	0.17769	9.26194E-4	0.99919
2.6	0.05571	0.77257	0.16417	7.23254E-4	0.99844
2.8	0.05542	0.72113	0.14074	5.67534E-4	0.99861
3	0.05532	0.66275	0.1118	4.38207E-4	0.9964
3.25	0.05185	0.6129	0.09752	3.25158E-4	0.99816
3.5	0.04959	0.57011	0.08175	2.45005E-4	0.99875
3.75	0.04764	0.53458	0.06953	1.85872E-4	0.99646
4	0.04405	0.50667	0.06881	1.41617E-4	0.99818
4.25	0.0402	0.4802	0.06919	1.07127E-4	0.99822
4.5	0.04007	0.45086	0.05169	8.0247E-5	0.99844
4.75	0.03891	0.43046	0.0484	6.07272E-5	0.99862
5	0.04011	0.40752	0.03439	4.56384E-5	0.99861
6	0.04991	0.34194	0.00774	1.60672E-5	0.99536
7	0.0782	0.29483	-0.02603	7.89165E-6	0.9984

Table S7. Best fitted parameters (χ_T, χ_S, τ and α) with the extended Debye model for compound **1@Zn** at 1200Oe in the temperature range 2-4.8 K.

T / K	χ_S / cm^3 mol^{-1}	χ_T / cm^3 mol^{-1}	α	τ / s	R^2
2	0.00426	0.0646	0.08477	0.02081	0.99858
2.2	0.00396	0.05883	0.06054	0.01198	0.99911
2.4	0.00432	0.05339	0.01511	0.00653	0.99029
2.6	0.00332	0.04945	0.03474	0.00388	0.99554
2.8	0.00294	0.04585	0.02876	0.00242	0.99369
3	0.00252	0.04258	0.0302	0.00154	0.99789
3.3	0.00216	0.03872	0.02764	8.81286E-4	0.99806
3.6	0.00281	0.03552	0.02047	5.47143E-4	0.9981

3.9	0.00293	0.03294	0.00321	3.59243E-4	0.99911
4.2	0.00259	0.03062	0.02404	2.37673E-4	0.99875
4.5	0.00755	0.02845	-0.06613	2.06985E-4	0.9994
4.8	1.09967E-4	0.0269	0.0392	1.05757E-4	0.99919

Table S8. Best fitted parameters (χ_T, χ_S, τ and α) with the extended Debye model for compound **2** at 3000Oe in the temperature range 2-8 K.

T / K	χ_S / cm^3 mol^{-1}	χ_T / cm^3 mol^{-1}	α	τ / s	R^2
2	0.07653	0.94494	0.32767	0.01452	0.99632
2.2	0.07213	0.80246	0.28299	0.00938	0.99755
2.4	0.07005	0.71369	0.23267	0.00674	0.99767
2.6	0.06271	0.70717	0.25144	0.0065	0.99685
2.8	0.05829	0.67489	0.23598	0.00564	0.99376
3	0.05812	0.64879	0.2074	0.0047	0.99113
3.25	0.05547	0.55237	0.15625	0.00311	0.99601
3.5	0.05138	0.54034	0.14921	0.00251	0.99823
3.75	0.05075	0.49233	0.10741	0.00166	0.99642
4	0.04501	0.49311	0.135	0.00121	0.99783
4.25	0.04232	0.45984	0.12138	7.46267E-4	0.99571
4.5	0.03955	0.43791	0.12183	4.7947E-4	0.99822
4.75	0.03802	0.41592	0.11928	3.07149E-4	0.99602
5	0.03711	0.39261	0.11182	2.013E-4	0.99402
6	0.03826	0.34236	0.11114	6.12126E-5	0.99748
7	0.04779	0.29703	0.05464	2.8595E-5	0.99529
8	0.05156	0.26367	0.01469	1.50582E-5	0.99621

Table S9. Best fitted parameters (χ_T, χ_S, τ and α) with the extended Debye model for compound **2** at 3000Oe in the temperature range 2-6 K.

T / K	χ_S / cm^3 mol^{-1}	χ_T / cm^3 mol^{-1}	α	τ / s	R^2
2	0.12631	0.88463	0.33756	0.00741	0.99581
2.2	0.11974	0.68694	0.25793	0.004	0.99358
2.4	0.11118	0.68153	0.24403	0.00368	0.99747
2.6	0.09711	0.67701	0.29236	0.00374	0.98815
2.8	0.09504	0.61356	0.23267	0.00282	0.99615
3	0.08966	0.57819	0.21092	0.00222	0.99795
3.25	0.08739	0.51166	0.14624	0.00158	0.98922
3.5	0.08013	0.49672	0.14828	0.00123	0.9874
3.75	0.07445	0.46005	0.12431	8.22446E-4	0.99201
4	0.0695	0.44741	0.12097	5.36688E-4	0.99565
4.25	0.0619	0.42025	0.12792	3.21355E-4	0.99108
4.5	0.06094	0.39802	0.10183	1.91846E-4	0.99045
4.75	0.05712	0.3793	0.09824	1.16346E-4	0.99671
5	0.05561	0.35971	0.08591	7.21785E-5	0.99401
6	0.04665	0.31714	0.10582	1.62696E-5	0.99353

Computational Details

All calculations were carried out using ORCA 5.0 suite of programs.[1] To extract the zero-field splitting parameters, g-value in complexes, we have prepared a monomeric model of both the complexes called $\mathbf{1}_{\mathbf{SeCN}}$, $\mathbf{2}_{\mathbf{Cl}}$ and $\mathbf{3}_{\mathbf{Br}}$ (see Figure S19). Next, we optimised the position of hydrogens using the BP86[2,3] level of theory with def2-SVP[4] basis set for all the atoms. The hydrogen optimised coordinates were used for the calculation of electronic, magnetic properties and spin-Hamiltonian parameters (g, D, E) of complexes $1a_{SeCN}$, $2a_{Cl}$ and $3c_{Br}$. These properties were computed by using the complete active space self-consistent (CASSCF)[5] method with an active space of CAS (7, 5) i.e., seven active electrons in the five active d-orbitals of Co(II). Using this active space, we have computed all the 10 quartets and 40 doublets states. All these calculations were carried out with a DKH-def2-TZVPP[4] basis set for all atoms. To treat the dynamic correlations, the second-order N-electron valence perturbation theory (NEVPT2)[6] method was employed on the converged CASSCF wavefunction. Ab-initio based ligand field theory (AILFT)[7] analysis was carried out to analyze the nature of ligand field and d-orbital splitting as implemented in ORCA.

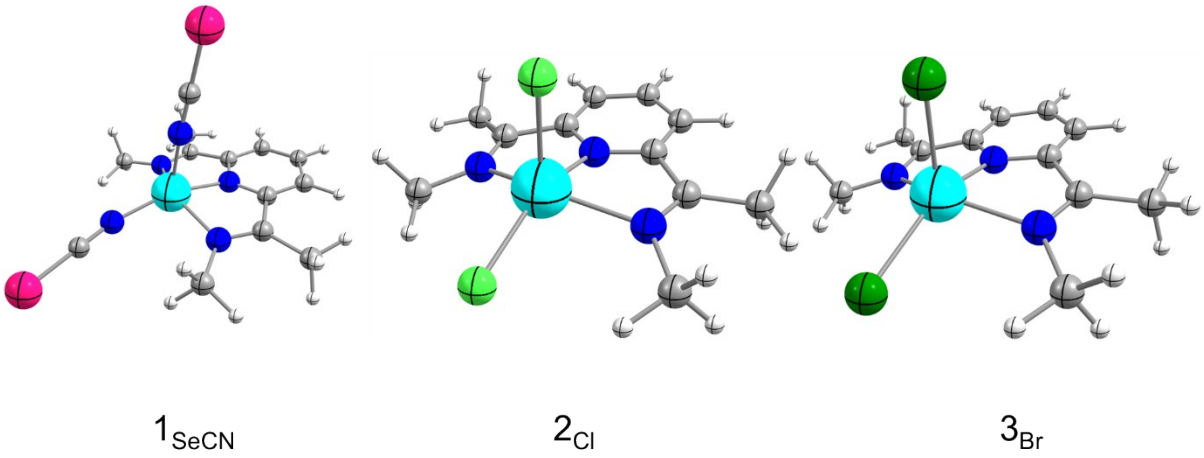

Figure S19: Hydrogen optimised model structures for complexes 1-3. The position of hydrogens was optimized using DFT calculations. Colour code: light blue, Co; dark blue, N; pink, Se; light green, Cl; dark green, Br; grey, C; white, H

Table S10.CASSCF (7,5)+NEVPT2 computed Spin–Hamiltonian parameter (g, D, |E/D|) parameters along with wavefunction decomposition analysis.

Parameters	1_{SeCN}		2_{Cl}		3_{Br}	
	CASSCF	NEVPT2	CASSCF	NEVPT2	CASSCF	NEVPT2
D	-65.52	-48.73	-74.56	-59.30	-61.21	-45.25
|E/D|	0.18	0.20	0.14	0.14	0.22	0.23
g_{xx}	2.054	2.066	2.073	2.084	2.078	2.093
g_{yy}	2.308	2.279	2.345	2.295	2.429	2.351
g_{zz}	2.936	2.761	3.073	2.895	2.976	2.775
KD1	62%|3/2; ±3/2⟩ + 36%|3/2; ±1/2⟩		64 %|3/2; ±3/2⟩ + 32%|3/2; ±1/2⟩		58 %|3/2; ±3/2⟩ + 38%|3/2; ±1/2⟩	
g_{xx}	0.999	1.090	0.851	0.826	1.183	1.213
g_{yy}	1.304	1.451	1.072	1.032	1.663	1.687
g_{zz}	8.459	7.927	8.913	8.448	8.448	7.884
KD2	60 %|3/2; ±3/2⟩ + 36%|3/2; ±1/2⟩		64 %|3/2; ±3/2⟩ + 30%|3/2; ±1/2⟩		56 %|3/2; ±3/2⟩ + 38%|3/2; ±1/2⟩	
g_{xx}	2.823	2.504	3.133	2.853	2.669	2.413
g_{yy}	3.368	3.145	3.698	3.605	3.314	3.069
g_{zz}	4.997	5.180	4.826	4.924	5.241	5.364

Table S11.AILFT derived ligand field parameters computed at NEVPT2 level of theory for model complexes **1-3**. The values of *B*, *C* and ξ parameters are provided in units of cm^{-1}

Parameter	Free Co(II)	1_{SeCN}	2_{Cl}	3_{Br}	% Reduction		
ξ	527	514.9	512.5	503.6	2.30	2.75	4.44
B	1042.3	977.3	1003.9	962.0	6.24	3.68	7.70
C	4156.5	3769.2	3921.0	3823.4	9.32	5.67	8.01
C/B	3.988	3.857	3.906	3.975	3.28	2.06	0.33
% Reduction =							

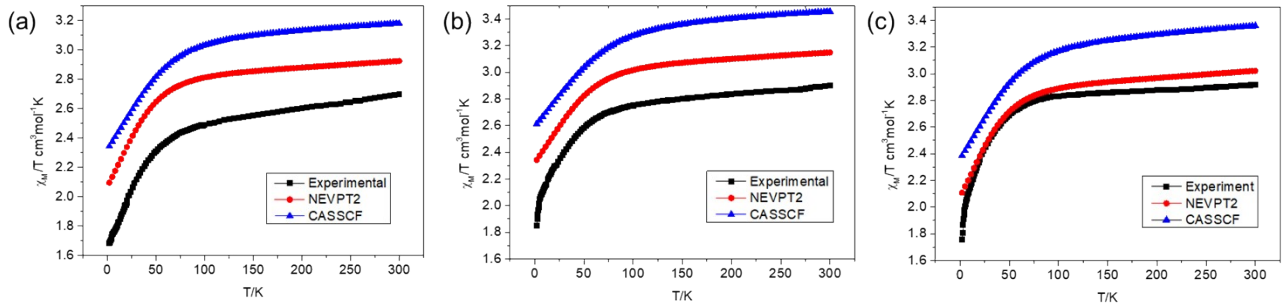

Figure S20: NEVPT2 computed magnetic susceptibility plots for complexes (a) 1_{SeCN}, (b) 2_{Cl} and (c) 3_{Br} where black squares correspond to the experimental values and the blue and red lines correspond to CASSCF and NEVPT2 computed values, respectively. All these computed values are obtained from the calculations on monomeric model complexes.

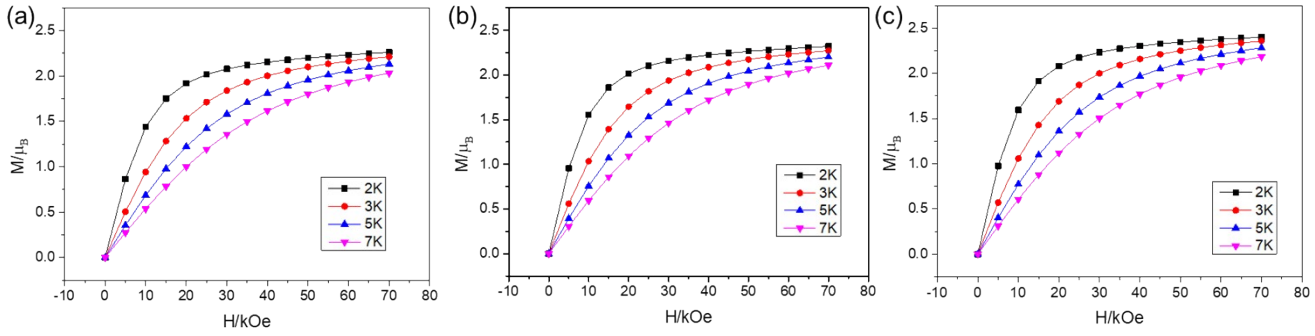

Figure S21. NEVPT2 computed magnetization curves for complexes (a) 1_{SeCN}, (b) 2_{Cl} and (c) 3_{Br}at 2K, 3K, 5K and 7K respectively. All these computed values are obtained from the calculations on monomeric model complexes.

Table S12.CASSCF/NEVPT2 computed 10 spin-free quartets (red) and 40 spin-free doublets (blue) states along with the spin-orbit states for complex 1_{SeCN}. All values are reported in cm^{-1}

SPIN-FREE STATES				SPIN-ORBIT STATES			
CASSCF		NEVPT2		CASSCF		NEVPT2	
0	35421.6	0	35307.2	0	31005.31	0	29750.13
792	45555	1129	39301.9	137.08	31376.39	103.31	30181.11
2395.3	45881.3	3053.6	40208.7	1000.84	31848.93	1282.93	30929.37
4310.1	46321.4	5465.5	40608.2	1182.11	32649.78	1425.64	31055.49
6965.9	47899.2	8753.8	42408.6	2576.59	33061.53	3174.07	31433.22
8127.9	47899.6	10148.3	42423.9	2659.17	33708.07	3258.03	32699.64
12452.6	48261.4	15590.9	43080.2	4575.74	34131.62	5663.6	32968.23
21063.9	48372.8	18493.5	43234.5	4701.52	34678.62	5771.05	33572.79
23690.3	69021.1	21744.6	59018.8	7185.76	34963.59	8900.19	34958.19
25754.1	69881.3	24080	60356.5	7255.44	35442.52	8945.3	35312.03
13971.2	71311.9	9393.9	62058.7	8346.85	36043.32	9623.49	35860.27
17644	72958.6	14470.7	63707.4	8460.46	45787.69	10297.32	39506.7
18211.8	73647.4	15099.7	64408.4	12765.3	46154.09	10417.84	40422.04
18930.1		15897		12782.36	46646.62	14693.77	40873.66
19972.1		18041.6		14198.97	48068.12	15286.33	42546.48
20677.3		18956.4		17911.55	48248.34	15780.57	42722.82
20751.7		18970.7		18435.26	48604.33	15836.28	43333.88
21494.1		19750.9		19219.16	48694.96	16213.13	43503.11
23644.6		21868		20128.67	69324.54	18156.2	59275.98
24216.6		21995.2		20966.01	70174.43	18591.29	60601.98
24980.7		22228.1		21110.18	71634.58	18654.94	62328.21
25649.2		22734.7		21245.17	73245.2	19182.59	63943.11
27675.6		25819.9		21288.06	73998.07	19305.21	64708.45
28442.5		26495.8		21809.46		20001.92	
28927.2		27054.3		23741.62		21519.14	
29316.9		27493.1		23817.89		21839.79	
30176.8		28792.9		23911.75		22075.43	
30633		29473.1		24515.09		22278.68	
31015.3		29890.7		25397.29		22741.34	
31527.9		30816.1		25887.25		23205.54	
32570.2		30862		26038.24		24270.96	
32608.8		31009.8		26277.42		24343.72	
33512.2		32556.3		27919.8		26014.84	
33847.2		32763.2		28676.06		26692.24	
34059.1		32984.1		29235.39		27322.99	
34604.5		34717.2		29674		27805.43	
35226.2		35190.7		30370.68		28957.56	

Table S13.CASSCF/NEVPT2 computed 10 spin-free quartets (red) and 40 spin-free doublets (blue) states along with the spin-orbit states for complex 2_{Cl}. All values are reported in cm^{-1}

SPIN-FREE STATES				SPIN-ORBIT STATES			
CASSCF		NEVPT2		CASSCF		NEVPT2	
0	44553.5	0	39808.9	0	29077.96	0	28463.06
628.9	44668.2	921.4	40201.4	153.46	29409.12	122.12	28785.33
2212.8	45151.9	3050.5	40926.6	873.19	29780.34	1113.13	28986.16
3058.6	46031.8	4245.6	41877.8	1080.47	30445.69	1278.27	29253.57
5567.4	46054.4	7217.2	41962.2	2388.24	30815.59	3171.97	29647.08
5873.7	46252.7	7625.6	42389.9	2483.51	31449.88	3257.4	31078.96
8715.3	46521.7	11329.5	42635.4	3385.26	31724.82	4488.7	31285.16
20392.9	68392.2	18343.9	60012.4	3571.05	32018.66	4638.09	31595.51
21999.8	68412.8	20710.9	60105.8	5781.51	32288.69	7368.91	31841.65
23227.2	69512.4	21738.8	61383.8	5863.23	32475.98	7438.48	32228.27
16453.2	70817.5	13377.9	63065.2	6159.44	33389.03	7840.2	33214.68
18549.4	71277.5	16666.7	63524.5	6349.52	44850.44	8003.49	40053.55
18858.8		16692.1		9113.44	44977.74	11629.68	40451.56
19129.4		17416.2		9149.01	45492.47	11653.86	41193.68
20079.9		18994.4		16675.73	46241.16	13586.65	42050.37
20168.2		19204.8		18775.97	46465.81	16761.17	42297.88
20364.5		19282.6		19132.49	46639.9	17048.09	42685.24
21182.7		20532.8		19454.87	46895.44	17670.58	42933.73
22238.1		21728.5		20266.7	68639.62	18484.48	60224.2
24143		22159.8		20576.87	68857.57	18532.8	60468.68
24502.7		22357.4		20616.49	69879.29	19124.36	61688.55
25516.3		23294.5		20674.97	71136.5	19485.59	63317.43
26774.3		25681.5		20791.63	71692.67	19676.18	63877.78
27402.5		26129.2		21504.24		20745.45	
27564.3		26343.5		22185.87		20815.78	
27874.1		26802.6		22266.5		20897.21	
28347.6		27827.5		22544.95		21561.85	
28531.9		28290.9		23344.16		21946.06	
29093.7		28356.6		23533.42		22210.89	
29331.9		28818.8		24524.56		22456.63	
30252.7		28849.8		25096.82		22973.63	
30358.6		29229.8		25932.03		23708.3	
31356.7		30990.3		27033.16		25865.05	
31383		31111.7		27603.34		26321.98	
31605.4		31129.1		27892.91		26665.95	
31708.6		31300.4		28287.55		27112.85	
31925.5		31953.1		28586.34		28021.78	
32696.3		32619.5					

Table S13**.** CASSCF/NEVPT2 computed 10 spin-free quartets (red) and 40 spin-free doublets (blue) states along with the spin-orbit states for complex 3_{Br}. All values are reported in cm^{-1}

SPIN-FREE STATES				SPIN-ORBIT STATES			
CASSCF		NEVPT2		CASSCF		NEVPT2	
0	32544	0	32075.6	0.00	29140.10	0.00	27899.21
741.8	44538.4	1113.2	38134.5	130.84	29510.92	97.48	28069.61
2026.4	44589.4	2874.7	38574	949.47	29784.17	1267.72	28523.45
2869	44928.1	4076	39099	1123.53	30518.18	1401.51	28766.47
5502.2	46144.7	7190.6	40403	2204.51	30862.18	2986.30	29283.03
5963.7	46170.3	7849.2	40435.3	2282.18	31239.84	3060.18	30261.88
8768.5	46332.5	11648.7	40828.3	3180.11	31602.27	4297.12	30527.34
20374	46530.1	17629.7	41020.1	3360.73	31876.09	4441.71	31009.76
21561.9	68097.1	19522.5	58112.7	5700.95	32232.45	7326.64	31223.81
23724	68194.5	21619.3	58307.5	5777.65	32423.93	7388.84	31717.82
16096.7	69732.8	12209.3	59937.2	6212.28	33218.52	8024.21	32620.37
18230.2	70731.2	15546.2	61270	6401.26	44798.61	8178.41	38351.99
18895.8	71466.4	16396.6	61992.8	9134.69	44873.89	11909.33	38791.06
19109.5		16476.6		9168.00	45260.19	11929.13	39349.03
19913.1		18281.8		16300.15	46335.42	12400.70	40538.24
20076		18569		18489.07	46523.09	15770.60	40739.73
20493.2		18884.2		19098.39	46711.56	16502.69	41105.32
21051.9		19725.1		19414.65	46878.25	16793.13	41289.31
22159.4		20914.5		20089.78	68366.09	17747.24	58338.39
23851.4		21540.7		20490.51	68568.63	17791.92	58599.59
24255.6		21568.8		20576.18	70064.59	18389.78	60207.59
25271.1		22449		20608.86	71045.15	18873.07	61514.66
26753.5		24578.9		20826.88	71835.33	19149.41	62297.34
27301.4		25346.2		21364.98		19603.96	
27841.3		25693.1		21741.92		19698.47	
27920.4		26080.7		21827.67		19969.49	
28392.3		27075.6		22430.09		20964.59	
28651.8		27623.4		23669.54		21577.91	
29242.1		27780.4		23961.69		21779.23	
29338.1		28269.6		24360.05		21939.95	
30344.9		28520.4		24846.85		22227.28	
30498.2		28977.1		25663.75		22837.21	
31077		30101.6		26990.10		24762.87	
31249.9		30344		27533.12		25519.34	
31467.9		30587.8		27984.21		25930.38	
31736.8		30743.8		28340.95		26380.98	
31959.9		31518.9		28672.42		27263.02	

References:

1 F. Neese, *Wiley Interdiscip. Rev. Comput. Mol. Sci.*, 2022, **e1606**, 1–15.

2 A. D. Becke, *Phys. Rev. A*, 1988, **38**, 3098–3100.

3 J. P. Perdew, *Phys. Rev. B*, 1986, **33**, 8822–8824.

4 F. Weigend and R. Ahlrichs, *Phys. Chem. Chem. Phys.*, 2005, **7**, 3297–3305.

5 P. Å. Malmqvist and B. o. Roos, *Chem. Phys. Lett.*, 1989, **155**, 189–194.

6 C. Angeli, R. Cimiraglia, S. Evangelisti, T. Leininger, J. Malrieu, C. Angeli and R. Cimiraglia, *J. Chem. Phys.*, 2014, **114**, 10252–10264.

7 M. Atanasov, D. Ganyushin, K. Sivalingam and F. Neese, in *Molecular Electronic Structures of Transition Metal Complexes II*, 2012, pp. 149–220.